Quantum kicked harmonic oscillator in contact with a heat bath

M. Á. Prado Reynoso,[1,2] P. C. López Vázquez,[3,4] and T. Gorin[1]

[1]*Departamento de Física, Universidad de Guadalajara, Boulevard Marcelino García Barragan y Calzada Olímpica, Codigo Postal 44840, Guadalajara, Jalisco, México*

[2]*Departamento de Física, Universidade do Paraná, 81531-980 Curitiba, Brazil*

[3]*Departamento de Ciencias Naturales y Exactas, Universidad de Guadalajara, Carretera Guadalajara-Ameca Km 45.5, Codigo Postal 46600, Ameca, Jalisco, México*

[4]*Max-Planck-Institut für Physik komplexer Systeme, D-01187 Dresden, Germany*

(Received 21 June 2016; published 17 February 2017)

We consider the quantum harmonic oscillator in contact with a finite-temperature bath, modeled by the Caldeira-Leggett master equation. Applying periodic kicks to the oscillator, we study the system in different dynamical regimes between classical integrability and chaos, on the one hand, and ballistic or diffusive energy absorption, on the other. We then investigate the influence of the heat bath on the oscillator in each case. Phase-space techniques allow us to simulate the evolution of the system efficiently. In this way, we calculate high-resolution Wigner functions at long times, where the system approaches a quasistationary cyclic evolution. Thereby, we perform an accurate study of the thermodynamic properties of a nonintegrable, quantum chaotic system in contact with a heat bath at finite temperature. In particular, we find that the heat transfer between harmonic oscillator and heat bath is governed by Fourier's law.

DOI: 10.1103/PhysRevA.95.022118

I. INTRODUCTION

Recently, the "emergence of thermodynamic behavior within composite quantum systems" [1] has become a very active research field. In this contribution, we study the thermodynamic properties of a quantum system coupled to a finite-temperature bath and how they are affected by the presence of "quantum chaos" [2,3] and different regimes of energy absorption.

Open quantum chaotic systems were studied initially in the form of the dissipative quantum kicked rotor [4–6], where the authors proposed and discussed different models for the coupling to environmental degrees of freedom. In these early works, the emphasis was on accurate description of the coupling to the environment and the observation of the destruction of dynamical localization due to decoherence. Later on, quantum chaos was investigated also on the side of the environment. There, the question was whether quantum chaos would imply special noticeable effects on the central system. This was studied, for instance, by comparing the effects of a particular quantum chaotic environment to the ubiquitous collection of harmonic oscillators [7–10]. Similarly, in the spirit of the quantum chaos conjecture [11–14], Lutz and Weidenmüller studied an environment modeled by random matrix theory [15].

Eventually, random matrix environments were used to describe decoherence [16–18] and quantum information processes [19–22] in open quantum systems. We also mention Ref. [23], which is actually one of the first papers on a random matrix approach to open quantum systems, which deals with the description of highly excited vibrational states in molecules.

However, such studies do not explain how a quantum chaotic environment can appear in an experimental setup. Of course, one may simply assume that system and quantum chaotic environment are perfectly isolated from anything else, but this is a rather unrealistic assumption. In practice, it is inevitable that the quantum chaotic environment will be in contact with other degrees of freedom not considered so far, the "far environment." Here, we assume the far environment acts as a finite-temperature reservoir. This allows us to study not only the equilibrium states of the quantum chaotic environment but also the relaxation processes towards those states. We believe that the nonequilibrium dynamics and the freedom to choose very strong or very weak couplings (in those cases, the canonical ensemble picture is not expected to work) open up new and interesting lines of research, where quantum chaos may lead to new effects.

In this work, we focus on energy flow between the system and environment and the adverse effects of decoherence on the ballistic energy absorption at quantum resonances. Thus, instead of studying a quantum chaotic system as it is coupled to an environment, which was the point of view in the early works, we study a system in thermodynamic equilibrium, as its dynamics become quantum chaotic. On this basis, we study to what extent Fourier's law describes the energy transfer from the chaotic system to the environment, acting as a heat bath at finite temperature.

One of the simplest examples of an open quantum system with well-defined canonical thermodynamic properties is the harmonic oscillator coupled to an environment which by itself consists of a continuous collection of oscillators [24,25], which can be described by the Caldeira-Leggett master equation [24,26]. Even though this equation is neither exact nor of Lindblad form, it is an excellent approximation as long as the temperature is not too low. In this model, the central harmonic oscillator evolves asymptotically into the canonical mixture of eigenstates with the corresponding Boltzmann weight factors. We then introduce quantum chaotic dynamics into the system by applying periodic kicks to the central harmonic oscillator. Without the environment, this system, the quantum kicked harmonic oscillator (KHO), has been studied in considerable detail, classically in Ref. [27] (for an introduction see [28,29] and references therein) and quantum mechanically [30–33]. The combination of a quite simple master equation and

periodic kicks which do not interfere with the dissipative dynamics allows numerical simulations to be done very efficiently without further approximations. The quantum KHO with dissipation was studied previously in Refs. [31,34]. It may be realized experimentally following [35]. In [31], the authors considered the two limiting cases of zero and infinite temperature. Also, they concentrated on the initial stage of the evolution, investigating the "breaking time" where the quantum evolution starts to deviate notably from the classical one. In Ref. [34] the author considers the same system at a quantum resonance and derives analytical expressions for the energy absorption with and without coupling to the heat bath.

The advantage of introducing quantum chaos with the help of a time-dependent potential and not via an additional degree of freedom lies in the reduced numerical requirements. The disadvantage lies in the fact that energy is no longer conserved. Thus, we cannot apply standard thermodynamical concepts such as the canonical ensemble when kicking is present. However, note that the thermodynamics of time-periodic systems has been treated in [36,37].

For the simulations we use the Fourier transform of the Wigner function of the system, which was called the "chord function" in Refs. [38,39]. We solve analytically for the chord function of the harmonic oscillator in contact with the heat bath and then apply a kick to the oscillator. By using interpolation techniques we are able to repeat this joint mapping of dissipative dynamics and unitary kicks, describing the full evolution of the system. We focus on the effects of the coupling to the thermal bath in different parameter regimes, such as on and off quantum resonances [32], as well as in transition regions, where the classical counterpart changes from integrable to chaotic [40].

The paper is organized as follows: In Sec. II we describe the model and the method applied to obtain our numerical simulations. Then, in Sec. III we present our simulations in two parts, the first concentrating on the equilibrium properties at relatively strong coupling to the heat bath and the second showing the reappearance of the dynamical properties of the closed system, when the coupling to the heat bath is reduced. Finally, in Sec. IV we present our conclusions.

II. THE MODEL

In this section, we introduce the quantum master equation, which describes the system of interest (Secs. II A and II B) and then describe our method to perform the numerical simulations (Secs. II C and II D).

A. Quantum master equation

Choosing a linear and separable coupling between the system and environment and restricting oneself to high temperatures, it is possible to derive the following quantum master equation:

$$i\hbar\frac{d\varrho}{dt} = [H_{\rm HO},\varrho] + \gamma\,[\hat{X},\{\hat{P},\varrho\}] - i\frac{2\gamma\, m k_{\rm B} T}{\hbar}\,[\hat{X},[\hat{X},\varrho]],$$
$$H_{\rm HO} = \frac{\hat{P}^2}{2m} + \frac{m\omega_{\rm o}^2}{2}\,\hat{X}^2. \qquad (1)$$

This equation was originally derived by Caldeira and Leggett [24] under the assumption that the environment consisted of a continuous collection of harmonic oscillators. Here, the central harmonic oscillator has mass m and angular frequency $\omega_{\rm o}$. The damping constant γ characterizes its relaxation rate, which is related to the Ohmic spectral density of the collection of harmonic oscillators in the environment. Finally, T is the equilibrium temperature of these oscillators, and $k_{\rm B}$ is the Boltzmann constant.

In order to add the periodic kicks to the system, we replace $H_{\rm HO}$ by

$$H_{\rm KHO} = H_{\rm HO} + K\cos(\mu\hat{X})\sum_{n\in\mathbb{Z}}\delta(t - n\,T_{\rm K}), \qquad (2)$$

where μ is the wave number of the kick potential. The kick strength and the time period between two kicks are denoted by K and $T_{\rm K}$, respectively.

When the kick strength dominates over the coupling to the heat bath, the system essentially behaves as the ordinary KHO where the evolution is unitary [32,33]. This model has a wide range of dynamical features. To study the different regimes, it is simplest to start with the relation between the fundamental period of the harmonic oscillator $2\pi/\omega_{\rm o}$ and the kick period $T_{\rm K}$. Their ratio,

$$q = \frac{2\pi}{\omega_{\rm o}\,T_{\rm K}}, \qquad (3)$$

may be rational or irrational, where the former generally leads to the formation of a unbounded "stochastic web" extending over the whole phase space. In the special cases $q = 1,2,3,4,6$ the stochastic web has a crystal symmetry; otherwise, it forms a quasicrystal structure. Apart from q, the system has two additional independent parameters, the kick wave number μ and the kick strength K. These two parameters define the overall scale for the dynamics in phase space and the degree of chaos. This will be worked out in more detail in Sec. II B. The degree of chaos is understood to mean the relative size of the areas occupied by the stochastic web vs the islands of integrable motion. While the overall scale does not make a difference for the classical dynamics, that is not so in the quantum case. There, the size of the primitive crystal cell may be compared to $\hbar$, such that a different size may lead to different dynamical behavior, such as the occurrence of "quantum resonances", mentioned in the introduction. Finally, as first discovered in the kicked rotor, one may also observe dynamical localization [41].

In the opposite case, when the coupling dominates over the periodic kicks ($K \approx 0$), the system becomes the quantum harmonic oscillator coupled to a heat bath in the high-temperature regime [25,26]. In this case, the system tends towards a thermal equilibrium state, following closely the dynamics of the classical damped harmonic oscillator (see Appendix B).

B. Dimensionless model

Choosing suitable units for position [$\hat{X} = \sqrt{\hbar/(m\omega_{\rm o})}\,\hat{x}$] and momentum ($\hat{P} = \sqrt{\hbar m\omega_{\rm o}}\,\hat{p}$), the master equation (1) is

rewritten as

$$i\frac{d\varrho}{d\tau} = [H_\kappa,\varrho] + \frac{\beta}{2}\,[\hat{x},\{\hat{p},\varrho\}] - i\beta\, D[\hat{x},[\hat{x},\varrho]], \qquad (4)$$

where energy is measured in units of $\hbar\omega_o$ such that $\hbar\omega_o\, H_\kappa = H_{\rm KHO}$ ($\hbar\omega_o\, H_0 = H_{\rm HO}$) and

$$H_\kappa = \frac{\hat{p}^2+\hat{x}^2}{2} + \frac{\kappa\,\cos(\sqrt{2}\,\eta\,\hat{x})}{\sqrt{2}\,\eta^2}\sum_{n\in\mathbb{Z}}\delta\left(\tau - 2\pi\,\frac{n}{q}\right), \qquad (5)$$

where q is the number of kicks per oscillator period, as defined in Eq. (3). Here, we have also introduced the dimensionless time $\tau = \omega_o t$ to describe the evolution of the system. The relative thermal energy is replaced by the dimensionless diffusion constant $D = k_B\,T/(\hbar\,\omega_o)$ from the quantum Brownian motion model, while $\beta = 2\gamma/\omega_o$ is the dimensionless energy decay rate. In what follows, we consider D to be a dimensionless temperature of the heat bath, described by the above master equation. Finally, the so-called Lamb-Dicke parameter [42] $\eta = \mu/\sqrt{2m\omega_o/\hbar}$ fixes the overall scale of the classical or quantum dynamics in phase space, while the effective kick strength $\kappa = K\mu^2/(\sqrt{2}\,m\omega_o)$ determines the degree of chaoticity in the classical system. In Eq. (5), the parameter η appears as an effective wave number in the cosine function of the kick potential. Thus, the larger η is, the smaller the scale of the classical structures in phase space is. Since we have chosen units such that quantum states occupy an average area of size 1, the role of $\hbar$ is here taken by η^2. Hence, the semiclassical limit corresponds to the limit $\eta^2 \to 0$.

In this work, we restrict ourselves to an integer number of $q = 4$ or 6 kicks per oscillator period. We then observe quantum resonances when η^2 is equal to an integer multiple of π. This resonance condition leads to a quadratic energy absorption; otherwise, the energy absorption is linear in time. The phenomenon, which was first discovered in the quantum kicked rotor [43], relies on the possibility to rewrite the Floquet operator for the evolution over q ν kicks under a kick strength κ as an evolution over only q kicks with an effective kick strength of $\kappa\,\nu$. In the KHO, the reason for that can be traced back to the commutation of certain displacement operators which describe a two-dimensional crystal lattice in phase space (for details, see Ref. [32]).

C. Dynamics

In general, the dynamics of the system is given in terms of two alternating autonomous quantum maps, Λ_β and Λ'. The first describes the dissipative dynamics under the Caldeira-Leggett master equation,

$$i\frac{d\varrho}{d\tau} = [H_0,\varrho] + \frac{\beta}{2}\,[\hat{x},\{\hat{p},\varrho\}] - i\beta\, D\,[\hat{x},[\hat{x},\varrho]], \qquad (6)$$

for the time $2\pi/q$ between two consecutive kicks. For $\beta > 0$, this map turns pure states into mixed states, which makes it necessary to describe the whole dynamics in the space of mixed states. The second map is a unitary transformation, which amounts to an instantaneous change in the momentum wave function of the system. Thus,

$$\Lambda_\beta\colon \varrho(0) \to \varrho(2\pi/q), \quad \Lambda'\colon \varrho \to \varrho' = U_\kappa\,\varrho\,U_\kappa^\dagger, \qquad (7)$$

where $\varrho(\tau)$ is a solution of the Caldeira-Leggett master equation and

$$U_\kappa = \exp\left[\frac{-i\kappa}{\sqrt{2}\eta^2}\,\cos(\sqrt{2}\eta\hat{x})\right]. \qquad (8)$$

For definiteness, let us agree to start always with the evolution Λ_β. Then, we obtain for the solution of Eq. (4) with the initial state ϱ_0:

$$\varrho_n^+ = \varrho(\tau_n^+) = (\Lambda'\circ\Lambda_\beta)^n\,\varrho_0, \qquad (9)$$

where the symbol $\circ$ means the composition of the two maps (the left one to be applied after the right one), while the nth power means the composition of n times the same map. This yields the state of the system right after the nth kick, i.e., at an infinitesimal time lapse after the time $\tau_n = 2\pi\,n/q$.

The Caldeira-Leggett master equation can be solved analytically in terms of the Fourier transform of the Wigner function [25,44,45]

$$\begin{aligned} w(k,s;\tau) &= \int_{-\infty}^{\infty}\int_{-\infty}^{\infty} dp\,dz\,e^{izk+isp}\,W(z,p;\tau) \\ &= \int_{-\infty}^{\infty} dz\,e^{izk}\,\langle z+s/2|\,\varrho(\tau)\,|z-s/2\rangle, \end{aligned} \qquad (10)$$

which has also been dubbed the "chord function" [38,39]. This function is normalized such that $w(0,0;\tau) = 1$ for all $\tau \geqslant 0$. In the second integral appears the mixed state $\varrho(\tau)$ in the position representation $\langle x|\,\varrho(\tau)\,|x'\rangle$ in Dirac notation. In the chord function representation, the Caldeira-Leggett equation becomes a first-order partial differential equation in the three variables k,s, and τ,

$$\partial_\tau w + (\beta s - k)\,\partial_s w + s\,\partial_k w = -D\beta s^2 w, \qquad (11)$$

which can be solved by the method of characteristics. The calculation, described in Appendix A, yields the following result:

$$w(\vec{r},\tau+\sigma) = w(\boldsymbol{M}(-\sigma)\vec{r},\tau)e^{-D\beta[\vec{r}^{\,T}\,\boldsymbol{A}(\sigma)\,\vec{r}\,]}, \qquad (12)$$

where a state at time τ with chord representation $w(\vec{r},\tau) = w(k,s;\tau)$ is mapped onto its image at time $\tau+\sigma$, with chord representation $w(\vec{r},\tau+\sigma)$. The matrices $\boldsymbol{M}(-\sigma) = \boldsymbol{M}(\sigma)^{-1}$ and $\boldsymbol{A}(\sigma)$ are given in Appendix A. There, one may convince oneself that $\boldsymbol{M}(\sigma)$, if transformed into ordinary phase space, describes the classical evolution of the damped harmonic oscillator with damping rate $\beta/2$. We may thus write for the action of Λ_β in this representation

$$\Lambda_\beta\colon w(\vec{r},\tau) \to w(\vec{r},\tau+2\pi/q). \qquad (13)$$

In order to complete the evolution of the system, we also need to describe the unitary map Λ' in the chord representation. A straightforward calculation, which first switches from the chord function to the position representation, then applies the kick according to Eqs. (7) and (8), and finally switches back to the chord-function representation, yields

$$\Lambda'\colon w(\vec{r},\tau) \to w'(\vec{r},\tau) = \sum_{l=-\infty}^{\infty}\mathcal{A}_l(s)\,w(\vec{r}_l,\tau), \qquad (14)$$

where $\vec{r}_l = (k - \sqrt{2}\eta\, l, s)$ and

$$\mathcal{A}_l(s) = (-1)^l\, J_l\left[\frac{\sqrt{2}\,\kappa}{\eta^2}\sin(\eta s/\sqrt{2})\right]. \tag{15}$$

In this expression, $J_l(z)$ is the Bessel function of the first kind [46]. Thus, the effect of the kick consists of generating a superposition of an infinite copies of the original chord function, each with a specific amplitude and displacement along the variable k.

D. Numerical implementation

The numerical implementation of the evolution of the system relies on the ability to accurately represent the true chord function of the evolving mixed quantum state and to accurately implement the two quantum maps Λ_β and Λ'. Our numerical approach consists of storing the chord function as a two-dimensional array of function values on an equally spaced grid in (k,s) space. Then, the application of Λ_β requires us to update the function values on each grid point according to Eq. (12). This step requires knowledge of the function values of the original state at points (k,s) in between the grid points. We estimate these values with the help of the bilinear interpolation method [47]. By contrast, the application of Λ' via Eq. (14) is easier. Since the s variable does not change, we need to perform only a one-dimensional interpolation on the displaced k variable. For simplicity (consistency) we choose a linear interpolation scheme in this case also.

With the chord function at hand, we use separable routines to calculate probability densities in position and momentum space, as well as expectation values of the first and second moments of position and momentum. Finally, we use the two-dimensional fast Fourier transform [47] to obtain the Wigner function representation. The simulations presented in this work are performed on a current workstation, using grids with up to 8000×8000 grid points.

III. SIMULATIONS

In this section we study the effect of the coupling to a heat bath on the quantum KHO [32]. This system has been thoroughly studied as a closed system, as it has an extremely rich range of interesting dynamical features [30–33]. However, much less is known about the open system with coupling to a heat bath; here, Refs. [31,34] are the only publications we are aware of.

The present work focuses on the equilibrium properties of the system and the validity of thermodynamic concepts in this regime. In Sec. III A, we thus start with the case of relatively strong coupling to the heat bath, where we expect that specific dynamical properties of the KHO to play only a minor role and where the equilibrium states are close to the thermodynamic equilibrium states of the harmonic oscillator without kicks. In Sec. III B, we reduce the coupling to the heat bath and observe the reappearance of different dynamical effects related to quantum chaos and quantum resonances.

A. Thermodynamical properties at strong coupling

In the quantum KHO any initial state normally tends to spread over the whole phase space, leading to ever higher energy expectation values $\langle H_{\rm HO}\rangle$. By contrast, when the system is coupled to a heat bath, one expects that $\langle H_{\rm HO}\rangle$ eventually saturates at a finite value. Accordingly, the evolution of the quantum states becomes periodic at large times, such that with each kick, the Wigner function expands in phase space (accompanied by an increase in energy) and relaxes again towards the equilibrium state of the Caldeira-Leggett model [see Eq. (B5) in Appendix B]. While this behavior is expected to happen for any finite coupling, it is difficult to observe when the coupling is small. This is because the regime of cyclic behavior is reached only at large times and large energies. In this section, we choose a rather large coupling $\beta = 0.1$, such that the cyclic regime is reached relatively quickly and hence easier to observe.

In Fig. 1 we present Wigner functions of evolving quantum states, starting out at $\tau = 0$ from the coherent state in the center of the phase space. We show the Wigner functions just after the 35th kick (first column), right before the 36th kick (second column) and right after the 36th kick (third column). At these times, the system is already very close to its limit cycle behavior in all the cases considered, as can be seen from Fig. 2. The first row shows the resonant case, with $\kappa = -0.8$ and $\eta^2 = \pi$, such that the kick amplitude is $\kappa/(\sqrt{2}\,\eta^2) \approx 0.18$. The second row shows the nonresonant case, with $\kappa = -0.8$ and $\eta^2 = 0.7\,\pi$, where $\kappa/(\sqrt{2}\,\eta^2) \approx 0.25$. The third row shows the chaotic case, with $\kappa = -4.5$ and $\eta^2 = 1$, where $\kappa/(\sqrt{2}\,\eta^2) \approx 3.18$. Remember, while κ determines the degree of classical

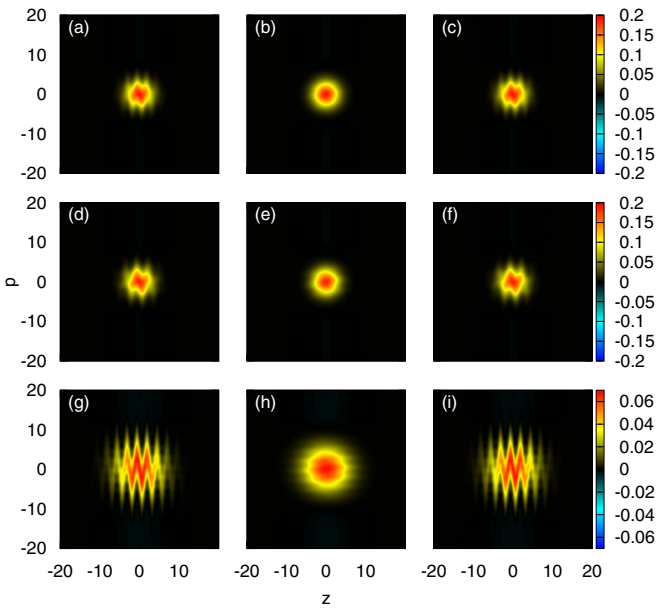

FIG. 1. Wigner function for the quantum KHO for $q = 4$, coupled to a heat bath (with $\beta = 0.1$ and $D = 5$), with an initial coherent state positioned at $z = 0, p = 0$. Different rows correspond to different choices of κ and η. Resonant case ($\kappa = -0.8, \eta^2 = \pi$) (a) after the 35th kick, (b) before the 36th kick, and (c) after the 36th kick. (d)–(f) Nonresonant case ($\kappa = -0.8, \eta^2 = 0.7\,\pi$) at the same instances in time. (g)–(i) Chaotic case ($\kappa = -4.5, \eta^2 = 1$).

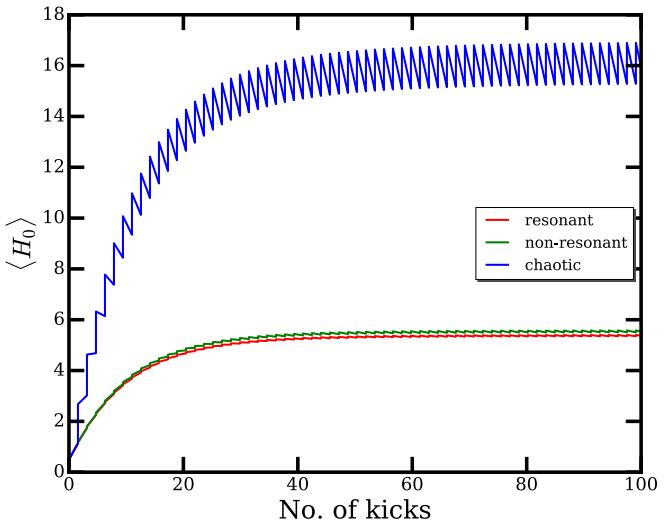

FIG. 2. Energy of the dimensionless harmonic oscillator $\langle H_0\rangle$ vs the number of kicks for the same three cases shown in Fig. 1. The lowest curve (red line) corresponds to the resonant case with $\kappa = -0.8$ and $\eta^2 = \pi$; the curve slightly above (green line) corresponds to the nonresonant case with $\kappa = -0.8$ and $\eta^2 = 0.7\pi$. The top curve (blue line) corresponds to the chaotic case with $\kappa = -4.5$ and $\eta^2 = 0.7\pi$.

chaos in the system, the size of classical structures in phase space is proportional to η^{-1}, while quantum states always occupy an average area of size 1.

Comparing the Wigner functions shown in the first and the second rows, we can hardly note any differences. This confirms the dominant effect of the coupling to the heat bath. Without coupling, i.e., for the closed KHO, we would expect a much more extended Wigner function in the resonant case (first row) than in the nonresonant case (second row). The Wigner functions in the third row correspond to the chaotic case. There, the Wigner functions are much more extended. However, this is mainly due to the different kick amplitudes as calculated in the previous paragraph (3.18 for the chaotic case vs. 0.18 and 0.25 for the resonant and nonresonant cases). The zigzag pattern, most clearly recognizable for the states right after a kick, can be directly related to the kick potential, as its periodicity in the z direction agrees with that of the kick potential.

In Fig. 2, we show the evolution of the (dimensionless) system energy $\langle H_0\rangle$ as a function of the number of kicks for the same three cases with $q = 4$ depicted in Fig. 1. As we chose the same initial state (a coherent state at the origin), the energy of the system starts out at $\langle H_0\rangle = 1/2$. The evolution starts out at $\tau = 0$ with a solution of the Caldeira-Leggett master equation. Initially, the energy of the system is smaller than the thermal energy $D = 5$ of the heat bath, and therefore, the system absorbs energy from the heat bath. After about 30 kicks, the system energy becomes larger than D, and therefore, the system releases energy to the heat bath. We observe that the two curves for the resonant and nonresonant cases are very close together, and they reach approximately the same final average energy, close to $D = 5$. This means that the effect of the kicks is weak compared to the heat bath. In the chaotic case (topmost blue line), one can clearly observe the effect of each individual kick and the subsequent relaxation. Here, the effect of the kicks is strong compared to the heat bath. Therefore, the average energy of the system increases to much larger values, varying finally around the value $\langle H_0\rangle \approx 16$. Figure 2 shows that the limit-cycle behavior is almost completely insensitive to the dynamical regimes of the isolated KHO. The only quantity which really matters is the kick amplitude $\kappa/(\sqrt{2}\,\eta^2)$ from Eq. (5), which determines the amount of energy transferred to the system at each kick.

Let us now turn our attention to the energy balance in the quasistationary regime. Specifically, we consider the energy of the harmonic oscillator, $E(\tau) = \langle H_0\rangle$, as a function of time τ. As far as time is concerned, we make use of the notation introduced in Sec. II C, where we denoted the time right after the nth kick by $\tau_n^+ = 2\pi\, n/q + \delta$ with an infinitesimal increment δ. Similarly, we denote τ_n^- as the time right before the nth kick. The quasistationary regime may thus be characterized by the condition that the whole energy $E(\tau_n^+) - E(\tau_n^-)$ gained from one kick is subsequently transferred to the heat bath during the time interval (τ_n^+, τ_{n+1}^-). In this process, the energy $E(\tau_n^-) = E(\tau_{n+1}^-)$ corresponds to the system state closest to equilibrium; we thus consider that energy the appropriate temperature scale.

$$D' = \lim_{n\to\infty} E(\tau_n^-). \tag{16}$$

On the other hand, taking the corresponding expectation values on both sides of the Caldeira-Leggett master equation, one can easily derive the following differential equation for expectation values:

$$\frac{d}{d\tau}\langle H_0\rangle = -\beta\,(\langle \hat{p}^2\rangle - D). \tag{17}$$

We approximate this formula at an instance right before the next kick. At this point, the system had time to equilibrate so that one may assume the equipartition theorem holds. In addition, we replace the derivative with a finite-time-difference quotient as follows:

$$\left.\frac{d}{d\tau}E(\tau)\right|_{\tau=\tau_n^-} \approx \frac{E(\tau_{n-1}^+) - E(\tau_n^-)}{2\pi/q} \approx -\beta[E(\tau_n^-) - D]. \tag{18}$$

In order to be valid, the time $2\pi/q$ between two kicks must be sufficiently short, such that the difference quotient is a reasonably good approximation of the derivative, and it must also be sufficiently long in order to allow the system to approach the equipartition condition, where $\langle H_0\rangle \approx \langle \hat{p}^2\rangle \approx \langle \hat{x}^2\rangle$.

At sufficiently long times, a quasistationary situation will be established, where the amount of energy added to the system due to the kicks is lost during the relaxation. We interpret the energy lost during relaxation as heat transferred to the environment at the dimensionless temperature D. Provided we identify D' from Eq. (18) as an effective temperature of the oscillator in the presence of kicks, the above equation becomes an instance of Fourier's law for the heat transport between the system and its environment at the different temperatures $D' > D$:

$$D' - D = \beta\,\frac{dQ}{d\tau}. \tag{19}$$

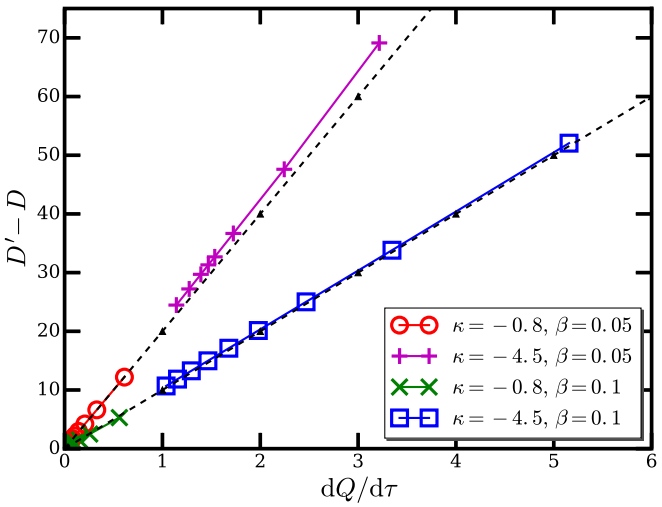

FIG. 3. Difference between the temperature of the system, measured by D' from Eq. (16), and the temperature of the heat bath vs the heat current $dQ/d\tau$ from Eq. (19) for $q=4$ and different KHO parameters κ and η^2, as well as coupling strengths β (see the legend). For each of the four cases, η^2/π varies from 0.2 to 1 in integer steps. Larger values of η^2 mean smaller kick amplitudes, and hence the corresponding points are closer to the origin. The black dashed lines show the theoretical expectation according to Fourier's law, Eq. (19).

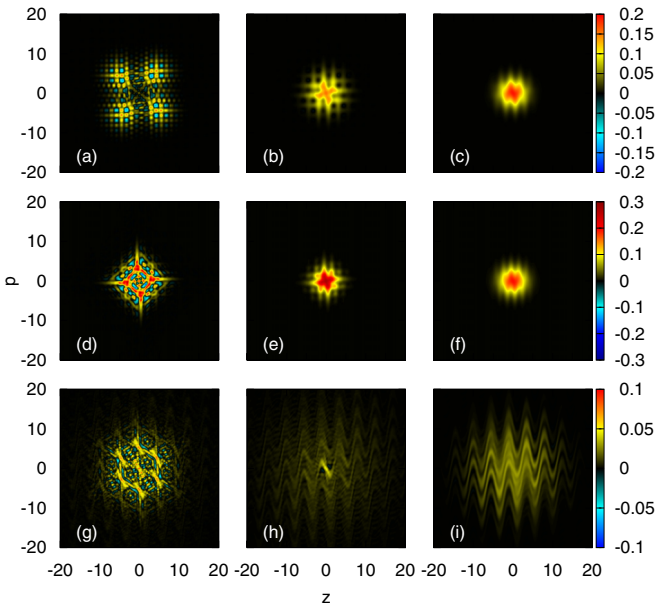

FIG. 4. Wigner functions right after the 36th kick for different coupling strengths: $\beta=0.001$ (first column), $\beta=0.01$ (second column), and $\beta=0.1$ (third column) for the resonant case (first row) with $q=4, \kappa=-0.8$, and $\eta^2=\pi$; the nonresonant case (second row) with $q=4, \kappa=-0.8$, and $\eta^2=(1+\sqrt{5})\pi/2$; and the chaotic case (third row) with $\kappa=-4.5$, $\eta^2=1$ but a kick period with $q=6$.

In Fig. 3, we study the amount of heat transferred to the reservoir as a function of the temperature (energy) difference $D'-D$, which may be interpreted as a temperature difference between the heat bath and the oscillator. This assumes that it is possible to assign a temperature to the oscillator in this quasiequilibrium situation. One then expects that Fourier's law (of thermal conduction) will hold, which predicts a linear relation between both quantities. Indeed, Fig. 3 confirms the validity of Fourier's law.

B. Weak coupling and reappearance of quantum chaotic and resonance properties

In Sec. III A, we studied the case of strong coupling to the heat bath, where different dynamical properties of the quantum KHO almost do not play any role. It is then natural to ask at which scales and how the different dynamical features reappear when the coupling to the heat bath is reduced. This is the purpose of the present section.

For the KHO, we have essentially three different parameters which can be changed: (i) the kick period $\tau_{n+1}-\tau_n=2\pi/q$, which may or may not be commensurable with the period 2π of the harmonic oscillator, (ii) the scale-invariant kick strength κ, which determines the degree of chaos in the corresponding classical system, and (iii) the scale (size) of the system in phase space, which is proportional to η^{-1}. As mentioned earlier, taking $\eta\to 0$ implements the semiclassical limit. However, η also controls the quantum resonances, where the system energy may increase quadratically in time, whereas, otherwise, the increase is only linear. For small coupling β, the study of the system is limited to a relatively narrow range of parameters or to short times. This is because our numerical scheme starts to fail if the Wigner functions become too extended in phase space. In those cases, it is increasingly difficult to reach the quasistationary regime.

In Fig. 4 we show Wigner functions after the 36th kick. Like in Fig. 1, we consider the resonant, nonresonant, and chaotic cases, each case in a different row. We vary the coupling strength from $\beta=0.001$ (first column) to $\beta=0.01$ (second column) and $\beta=0.1$ (third column). The case shown in the first row agrees with the resonant case in Fig. 1. The case in the second row differs in the value of η^2, while the chaotic chase in the third row corresponds to a different kick period with $q=6$. In the third column, where β is sufficiently large ($\beta=0.1$), the quasistationary regime is almost reached, and we can observe a behavior qualitatively similar to that in Fig. 1. Note, however, the larger extension of the quasistationary state in the chaotic case. For small values of β (first column), we find regions where the Wigner function represents relatively pure states with alternating regions of positive and negative values (which can be better appreciated by enlarging the plots). This is a signature of the state being nonclassical. For $\beta=0.001$ and 0.01, we also observe that the extension of the Wigner function is larger for the resonant case than for the nonresonant case, as expected according to the quadratic over linear energy absorption. That is no longer the case for $\beta=0.1$, where the quantum resonance condition seems to become meaningless, as discussed already in Fig. 2. In the chaotic case, the extension of the Wigner function is by far largest. As explained in Fig. 1, this is a simple consequence of the large kick amplitude. In the chaotic case, one would expect a linear increase in energy, just as in the nonresonant case [33]. The hexagonal symmetry observable for $\beta=0.001$ is due to the choice of $q=6$. It disappears as β is increased, until at $\beta=0.1$ the characteristic zigzag shape appears, just as in Fig. 1.

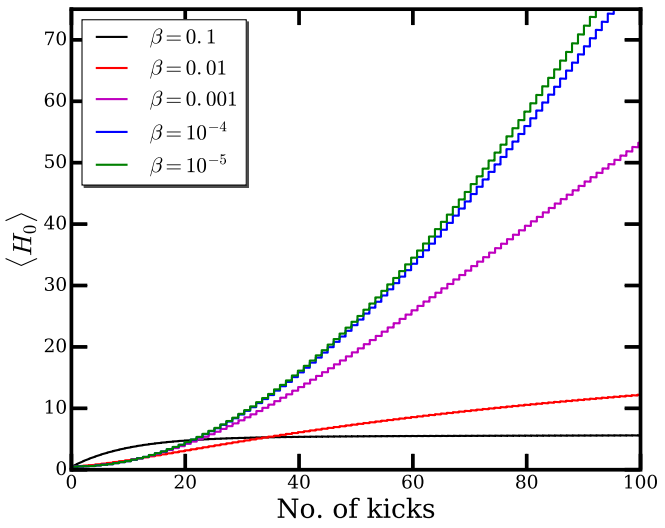

FIG. 5. Energy evolution in time in the resonant case, $q = 6$, $\kappa = -0.8, \eta^2 = 2\pi/\sqrt{3}$, for different coupling strengths from $\beta = 10^{-5}$ to $\beta = 0.1$. The increase in energy shown by the different curves is slower the larger β is.

In Fig. 5 the expectation value of the oscillator energy is shown as a function of the number of kicks applied to the system. The parameters for the KHO ($q = 4, \kappa = -0.8$, $\eta^2 = \pi$) are chosen to be the same as for one of the two resonant cases shown in Fig. 3(b) of Ref. [32], where the quantum KHO is treated without dissipation. Indeed, our result for $\beta = 10^{-5}$ seems to agree very well with the result shown there. We can clearly see the quadratic increase in energy, which becomes only slightly diminished when β is increased to $\beta = 10^{-4}$. By contrast, for the largest coupling, $\beta = 0.1$, the energy increases only in an initial phase and then quickly approaches its limit (average) value of $\langle H_0 \rangle \approx D = 5$. For intermediate couplings, $\beta = 0.001$ and $\beta = 0.01$, the quasistationary regime sets in only after many more kicks than could be shown here.

In Fig. 6 we plot the number of kicks required to reach the energy of $\langle H_0 \rangle = 50$. Again, this is done for $q = 4$, $\kappa = -0.8$. This time η is varied in a small region around the quantum resonance condition $\eta^2 = \pi/2$. This corresponds to the second case of a quantum resonance considered in Ref. [32]. We plot the number of kicks required to reach the above-mentioned energy limit as a function of η^2 for different coupling strengths from $\beta = 10^{-6}$ to $\beta = 0.01$. For the smallest coupling strength, we find the expected minimum, and we again confirm good agreement with the corresponding result in Fig. 3(a) from Ref. [32]. For increasing β, the minimum remains at its place, approximately until $\beta \approx 0.004$, and then disappears. At the largest coupling, $\beta = 0.01$, the number of kicks required to reach the energy limit becomes a monotonous function of η^2. It is noteworthy that increasing the coupling from $\beta = 10^{-6}$ to $\beta = 10^{-5}$ already leads to notable differences but only sufficiently far away from the quantum resonance. It is also interesting that for fixed $\eta^2 \approx 0.575\,\pi$, the number of kicks required does not increase monotonously with β. This phenomenon of a larger energy gain while increasing the coupling to the heat bath might be related to the reduction of dynamical localization due to decoherence [33,41].

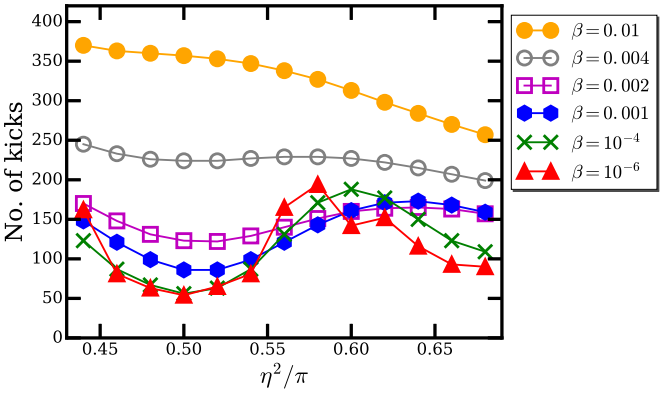

FIG. 6. Plots of the number of kicks required to reach a mean energy of $\langle H_0 \rangle = 50$ for the resonant case (with $\kappa = -0.8, q = 4$) and different coupling strength values β; the resonance is in $\eta^2/\pi = 0.5$.

IV. CONCLUSIONS

In this paper, we considered the quantum kicked harmonic oscillator as an open quantum system coupled to a finite-temperature heat bath. We studied its equilibrium properties at relatively strong coupling and found that, there, the system fulfills fundamental thermodynamic properties such as Fourier's law for heat transport. When reducing the coupling to the heat bath, the system's equilibrium state (i.e., its Wigner function representation) becomes ever more extended in phase space, and the expectation value of the oscillator energy increases. This makes it ever more difficult to perform simulations for a long time (many kicks), and eventually, we are no longer able to reach the equilibrium state. Thus, for small coupling, we restrict ourselves to studying the effect of quantum resonances and how it becomes suppressed and eventually eliminated due to the increasing coupling to the heat bath.

The numerical method is limited essentially by the requirement of an accurate representation of the chord function. At the present stage, we use a simple uniform two-dimensional grid together with a bilinear interpolation [47]. However, we are confident that this scheme can be improved in order to reach higher energies and larger times.

As shown in Ref. [35], the model is realizable experimentally in a quantum optical setup. Alternatively, one might think of ions in a harmonic trap. The coupling of the ion movement to its internal electronic states opens a way to consider the KHO with heat bath as a composite environment for a central quantum system. The reduced dynamics in the internal ion states may then serve as a probe for the thermodynamical properties of the KHO.

ACKNOWLEDGMENTS

We thank A. Eisfeld and F. Leyvraz for enlightening discussions. We acknowledge the hospitality of the Centro Internacional de Ciencias, UNAM, where some of the discussions took place. We are grateful for the possibility to use the computer cluster at the Max Planck Institute for the Physics of Complex Systems, where some of the numerical calculations

were performed. Finally, we acknowledge financial funding from CONACyT through Grant No. CB-2009/129309 at an early stage of the project.

APPENDIX A: SOLUTION OF THE CALDEIRA-LEGGETT MASTER EQUATION

Using dimensionless variables, the Caldeira-Leggett master equation for the harmonic oscillator transformed into the chord-function representation reads

$$\partial_\tau w + (\beta s - k)\partial_s w + s\partial_k w = -D\beta s^2 w, \tag{A1}$$

where $w = w(\vec{r},\tau)$ and $\vec{r} = (k,s)$. This is a first-order partial differential which can be solved with standard procedures. By the method of characteristics, it is turned into a system of ordinary differential equations

$$\frac{ds}{d\tau} = \beta s - k, \quad \frac{dk}{d\tau} = s, \quad \frac{dw}{d\tau} = -D\beta s^2 w, \tag{A2}$$

where the first two equations describe the characteristic curves in the (k,s) plane, along which the value of the chord function w changes with time according to the last. For the characteristics, we obtain the solution

$$\begin{aligned} k(\tau) &= e^{\beta\tau/2}\,(a_1\,\sin\omega\tau + a_2\,\cos\omega\tau), \\ s(\tau) &= \frac{d}{d\tau}\,k(\tau), \end{aligned} \tag{A3}$$

with $\omega = \sqrt{1-\beta^2/4}$ (valid for $\beta < 2$). The determination of the constants a_1 and a_2 is such that $k(0) = k_0$ and $s(0) = s_0$. Thereby, we construct the map $\boldsymbol{M}(\tau)$, which describes the motion of any point (k_0,s_0) along the characteristics. Because the system in Eq. (A2) is autonomous, we find $\vec{r}_{\tau+\sigma} = \boldsymbol{M}(\sigma)\,\vec{r}_\tau$, with

$$\boldsymbol{M}(\sigma) = e^{\beta\sigma/2}\begin{pmatrix} \cos\omega\sigma - \frac{\beta}{2\omega}\sin\omega\sigma & \frac{1}{\omega}\sin\omega\sigma \\ \frac{-1}{\omega}\sin\omega\sigma & \cos\omega\sigma + \frac{\beta}{2\omega}\sin\omega\sigma \end{pmatrix}. \tag{A4}$$

The map is invertible, and $\boldsymbol{M}(\sigma)^{-1} = \boldsymbol{M}(-\sigma)$. Furthermore, due to the prefactor $e^{\beta\sigma/2}$, the characteristics connect any point in the (k,s) plane with the origin as time goes to infinity.

Integration of the third equation in Eq. (A2) yields

$$\int_{w(\tau)}^{w(\tau+\sigma)} \frac{dw}{w} = -D\beta\int_\tau^{\tau+\sigma} d\tau'\,s^2(\tau'), \tag{A5}$$

where $w(\tau) = w(\vec{r}(\tau),\tau)$. For the integrand on the right-hand side, we find

$$s(\tau') = M_{21}(\tau'-\tau)\,k(\tau) + M_{22}(\tau'-\tau)\,s(\tau),$$

such that

$$\begin{aligned} &\int_\tau^{\tau+\sigma} d\tau'[M_{21}(\tau'-\tau)\,k(\tau) + M_{22}(\tau'-\tau)\,s(\tau)]^2 \\ &\quad = \int_0^\sigma d\sigma'[M_{21}(-\sigma')\,k(\tau+\sigma) + M_{22}(-\sigma')\,s(\tau+\sigma)]^2, \end{aligned} \tag{A6}$$

where we related the evolution along the characteristic to its end point. With this, we can write down an explicit expression for the evolution of the chord function from some initial time τ to an arbitrary final time $\tau+\sigma$:

$$w(\vec{r},\tau+\sigma) = w(\boldsymbol{M}(-\sigma)\vec{r},\tau)\exp[-D\beta\vec{r}^{\,T}\boldsymbol{A}(\sigma)\vec{r}], \tag{A7}$$

where the matrix elements of $\boldsymbol{A}(\sigma)$ are given by

$$\begin{aligned} A_{11}(\sigma) &= \int_0^\sigma d\sigma'\,M_{21}^2(-\tau'), \\ A_{12}(\sigma) &= \int_0^\sigma d\sigma'\,M_{21}(-\tau')M_{22}(-\tau') = A_{21}(\sigma), \\ A_{22}(\sigma) &= \int_0^\sigma d\sigma'\,M_{22}^2(-\tau'). \end{aligned} \tag{A8}$$

APPENDIX B: STATIONARY STATE

Without kicks, the system relaxes to the equilibrium state of the Caldeira-Leggett model. This state is easily obtained from the general evolution equation (A7) in the chord-function representation. Taking the limit $\sigma\to\infty$, one finds for an arbitrary initial chord function at $\tau = 0$

$$\lim_{\sigma\to\infty} w(\boldsymbol{M}(-\sigma)\vec{r},0) = w(\vec{o},0) = 1 \tag{B1}$$

due to the normalization of the Wigner function [see text below Eq. (10)]. At the same time, we obtain for the matrix $\boldsymbol{A}(\sigma)$

$$\lim_{\sigma\to\infty}\boldsymbol{A}(\sigma) = \frac{1}{2\beta}\begin{pmatrix} 1 & 0 \\ 0 & 1 \end{pmatrix}. \tag{B2}$$

This yields

$$w_{\rm ths}(\vec{r}) = \lim_{\sigma\to\infty} w(\vec{r},\sigma) = e^{-D\,(k^2+s^2)/2}. \tag{B3}$$

Transformation of $w_{\rm ths}(\vec{r})$ into the dimensionless position representation yields the following density matrix:

$$\varrho_{\rm ths}(x,x') = \frac{1}{\sqrt{2\pi D}}e^{-\frac{1}{8D}(x+x')^2 - \frac{D}{2}(x-x')^2}. \tag{B4}$$

The Wigner function of the system at the thermal state has the following form:

$$W_{\rm ths}(z,p) = \frac{1}{2\pi D}\exp\left(-\frac{z^2+p^2}{2D}\right), \tag{B5}$$

which is a two-dimensional Gaussian function centered at the origin with variance D in position and momentum. From this it follows for the expectation value of the energy $\langle H_0\rangle = (\langle z^2\rangle + \langle p^2\rangle)/2 = D$, the internal energy of the harmonic oscillator in thermal equilibrium. It corresponds to the temperature $T = (\hbar w_o/k_{\rm B})\,D$, in agreement with the definition of D below Eq. (5). Note that Eq. (B5) converges to the canonical equilibrium state of the harmonic oscillator only in the high-temperature regime [25,26].

[1] J. Gemmer, M. Michel, and G. Mahler, *Quantum Thermodynamics: Emergence of Thermodynamic Behavior within Composite Quantum Systems*, 2nd ed., Lecture Notes in Physics Vol. 784 (Springer, Berlin, 2009).

[2] H.-J. Stöckmann, *Quantum Chaos: An Introduction* (Cambridge University Press, Cambridge, 1999).

[3] F. Haake, *Quantum Signatures of Chaos*, 2nd ed. (Springer, Berlin, 2001).

[4] T. Dittrich and R. Graham, Ann. Phys. (NY) **200**, 363 (1990).

[5] D. Cohen, Phys. Rev. A **44**, 2292 (1991).

[6] D. Cohen, J. Phys. A **27**, 4805 (1994).

[7] M. Srednicki, Phys. Rev. E **50**, 888 (1994).

[8] D. Cohen, Phys. Rev. Lett. **78**, 2878 (1997).

[9] D. Rossini, G. Benenti, and G. Casati, Phys. Rev. E **74**, 036209 (2006).

[10] K. M. Fonseca Romero, J. E. Parreira, L. A. M. Souza, M. C. Nemes, and W. Wreszinski, J. Phys. A **41**, 115303 (2008).

[11] M. V. Berry and M. Tabor, Proc. R. Soc. London, Ser. A **356**, 375 (1977).

[12] G. Casati, F. Valz-Gris, and I. Guarneri, Lett. Nuovo Cimento **28**, 279 (1980).

[13] O. Bohigas, M.-J. Giannoni, and C. Schmit, Nonlinearity **8**, 203 (1995).

[14] R. Blümel and U. Smilansky, Phys. Rev. Lett. **64**, 241 (1990).

[15] E. Lutz and H. A. Weidenmüller, Phys. A (Amsterdam, Neth.) **267**, 354 (1999).

[16] M. Esposito and P. Gaspard, Europhys. Lett. **65**, 742 (2004).

[17] T. Gorin and T. H. Seligman, J. Opt. B **4**, S386 (2002).

[18] T. Gorin and T. H. Seligman, Phys. Lett. A **309**, 61 (2003).

[19] C. Pineda, T. Gorin, and T. H. Seligman, New J. Phys. **9**, 106 (2007).

[20] T. Gorin, C. Pineda, H. Kohler, and T. H. Seligman, New J. Phys. **10**, 115016 (2008).

[21] F. David, J. Stat. Mech. (2011) P01001.

[22] M. Carrera, T. Gorin, and T. H. Seligman, Phys. Rev. A **90**, 022107 (2014).

[23] W. M. Gelbart, S. A. Rice, and K. F. Freed, J. Chem. Phys. **57**, 4699 (1972).

[24] A. O. Caldeira and A. J. Leggett, Phys. A (Amsterdam, Neth.) **121**, 587 (1983).

[25] H.-P. Breuer and F. Petruccione, *The Theory of Open Quantum Systems* (Oxford University Press, Oxford, 2002).

[26] F. M. Ramazanoglu, J. Phys. A **42**, 265303 (2009).

[27] A. Chernikov, R. Sagdeev, and G. Zaslavsky, Phys. D (Amsterdam, Neth.) **33**, 65 (1988).

[28] L. E. Reichl, in *The Transition to Chaos: Conservative Classical Systems and Quantum Manifestations* (Springer, New York, 1992), pp. 156–221.

[29] G. Zaslavsky, Phys. Rep. **371**, 461 (2002).

[30] S. A. Gardiner, J. I. Cirac, and P. Zoller, Phys. Rev. Lett. **79**, 4790 (1997).

[31] A. R. R. Carvalho, R. L. de Matos Filho, and L. Davidovich, Phys. Rev. E **70**, 026211 (2004).

[32] T. P. Billam and S. A. Gardiner, Phys. Rev. A **80**, 023414 (2009).

[33] G. A. Kells, J. Twamley, and D. M. Heffernan, Phys. Rev. E **70**, 015203 (2004).

[34] M. D'Acunto, Rend. Semin. Fac. Sci. Univ. Cagliari **72**, 109 (2002).

[35] G. B. Lemos, R. M. Gomes, S. P. Walborn, P. H. Souto Ribeiro, and F. Toscano, Nat. Commun. **3**, 1211 (2012).

[36] R. Ketzmerick and W. Wustmann, Phys. Rev. E **82**, 021114 (2010).

[37] M. Langemeyer and M. Holthaus, Phys. Rev. E **89**, 012101 (2014).

[38] A. M. O. de Almeida, Phys. Rep. **295**, 265 (1998).

[39] A. M. O. de Almeida, J. Phys. A **36**, 67 (2003).

[40] M. Á. Prado Reynoso, master's thesis, Universidad de Guadalajara, 2016.

[41] M. Frasca, Phys. Lett. A **231**, 344 (1997).

[42] D. J. Wineland, C. Monroe, W. M. Itano, D. Leibfried, B. E. King, and D. M. Meekhof, J. Res. Natl. Inst. Stand. Technol. **103**, 259 (1998).

[43] G. Casati, B. V. Chirikov, F. M. Izraelev, and J. Ford, in *Stochastic Behavior in Classical and Quantum Hamiltonian Systems: Volta Memorial Conference, Como, 1977*, edited by G. Casati and J. Ford (Springer, Berlin, 1979), pp. 334–352.

[44] S. M. Roy and A. Venugopalan, arXiv:quant-ph/9910004.

[45] L. A. M. Souza, J. G. P. Faria, and M. C. Nemes, Opt. Commun. **331**, 148 (2014).

[46] *Handbook of Mathematical Functions*, edited by M. Abramowitz and I. A. Stegun (Dover, New York, 1970).

[47] *Numerical Recipes in Fortran*, edited by W. H. Press (Cambridge University Press, Cambridge, 1992).